Digit somatotopy in the human cerebellum: A 7 T fMRI study

Wietske van der Zwaag [a,b,*], Remy Kusters [b], Arthur Magill [a,b], Rolf Gruetter [a,b,c], Roberto Martuzzi [d,e], Olaf Blanke [d,e], José P. Marques [a]

[a] Department of Radiology, University of Lausanne, Switzerland
[b] Laboratory for Functional and Metabolic Imaging (LIFMET), Ecole Polytechnique Fédérale de Lausanne, Switzerland
[c] Department of Radiology, University of Geneva, Switzerland
[d] Laboratory of Cognitive Neuroscience (LNCO), Brain Mind Institute, Ecole Polytechnique Fédérale de Lausanne, Switzerland
[e] Center for Neuroprosthetics, School of Life Sciences, Ecole Polytechnique Fédérale de Lausanne, Switzerland

ARTICLE INFO

ABSTRACT

The representation of the human body in the human cerebellum is still relatively unknown, compared to the well-studied homunculus in the primary somatosensory cortex. The investigation of the body representation in the cerebellum and its somatotopic organisation is complicated because of the relatively small dimensions of the cerebellum, compared to the cerebrum. Somatotopically organised whole-body homunculi have previously been reported in both humans and rats. However, whether individual digits are represented in the cerebellum in a somatotopically organised way is much less clear. In this study, the high spatial resolution and high sensitivity to the blood oxygenation level dependent (BOLD) signal of 7 T fMRI were employed to study the BOLD responses in the human cerebellum to the stroking of the skin of individual digits, the hand and forearm.

For the first time, a coarse somatotopic organisation of the digits, ordered from D1–D5, could be visualised in individual human subjects in both the anterior (lobule V) and the posterior (lobule VIII) lobes of the cerebellum using a somatosensory stimulus. The somatotopic gradient in lobule V was found consistently in the posterior to anterior direction, with the thumb most posterior, while the direction of the somatotopic gradient in lobule VIII differed between subjects. No somatotopic organisation was found in Crus I. A comparison of the digit patches with the hand patch revealed that the digit regions are completely covered by the hand region in both the anterior and posterior lobes of the cerebellum, in a non-somatotopic manner. These results demonstrate the promise of ultra-high field, high-resolution fMRI for studies of the cerebellum.

Introduction

Digit somatotopy in the primary somatosensory cortex has recently been demonstrated at ultra-high field (Martuzzi et al., 2012; Sanchez-Panchuelo et al., 2010; Stringer et al., 2011), but digit mapping in the cerebellum, while more challenging because of the spatial dimensions, is also of interest because of the importance of the cerebellum in the somatosensory-motor feedback loop (Granziera et al., 2009; Lu et al., 2007). Anatomically, the cerebellum is divided in three lobes, which in turn are further subdivided into lobules (Schmahmann et al., 1999). The anterior lobe contains lobules I–V, the posterior lobe lobules VI–IX and the flocculonodular lobe contains lobule X (Fig. 1A). Lobule VII is again subdivided into Crus I, Crus II and lobule VIIB. Lobules I–V in the anterior lobe and lobule VIII in the posterior lobe are involved in

sensorimotor tasks (Manto et al., 2012; Stoodley and Schmahmann, 2009, 2010).

Somatotopic body representations were first found in lobules IV–VI in Rhesus monkeys (Adrian, 1943) and subsequently in lobule VIII in cats (Snider and Stowell, 1944). These early cerebellar somatotopy experiments already reported that some neurons in the cerebellum have very small receptive fields on the body — as small as the side of a single toe in a monkey (Adrian, 1943) or individual whiskers in rats (Shambes et al., 1978). In rats, large parts of the cerebellar "homunculus" are dedicated to the whiskers because of their importance for exploratory actions (Shambes et al., 1978). The importance of the digits for human exploratory action suggests that the human cerebellar digit representations will also be relatively large compared to their actual physical size.

Somatosensory mapping of the digit representations in the cerebellum with fMRI has not been frequently attempted because of the relatively small size of the cerebellum, the high level of foliation, which emphasizes inter-subject variability and complicates group studies, and the small size of the finger representations compared to those found in the primary somatosensory cortex. In addition to the high level of foliation, the cerebellar grey matter layer is 3–5 fold thinner than the cerebral grey matter sheet (Marques et al., 2010b), further complicating
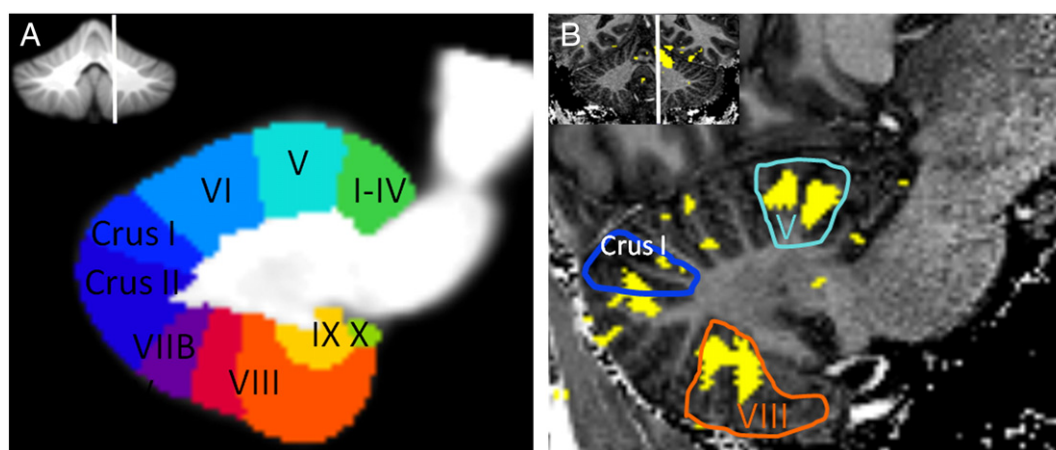
Fig. 1. Anatomy of the cerebellum. A: a sagittal slice from the SUIT toolbox with the individual lobules shown in colour (Diedrichsen, 2006). The insert shows the position of the sagittal slice with a white line on a coronal slice. B: an equivalent slice of an anatomical from an example subject with the activation mask overlaid (f-test over stroking of all digits, p<0.001). The three lobules of interest (V, VIII and Crus I) are outlined in the same colour as in panel A. Activation, shown in yellow, was found in lobule V, lobule VIII and Crus I. For this subject (#4 in Fig. 2), the Crus I activation spilled somewhat into Crus II.

comparisons across individuals. The spatial resolution at which the cerebellar homunculus is studied is important because the body representation is somatotopically organised at a coarse spatial resolution (Adrian, 1943; Buckner et al., 2011), but presents a more fractured organisation at sub-millimeter scales (Shambes et al., 1978). The term fractured somatotopy is used to indicate that the homunculus is broken up into small, patchy representations (Rijntjes et al., 1999). In fMRI, body representations have been defined as activation patterns that contain information about the represented body part (Diedrichsen et al., 2012). With the spatial resolution of a typical fMRI experiment, the fractured nature of the cerebellar body representation and the individual cerebellar folia cannot be accurately captured. To accurately resolve the fractured somatotopy pattern in the rat cerebellum, Shambes et al. needed 65 electrode punctures per mm, a 50-fold higher spatial resolution than that of the current fMRI experiments. With high-resolution fMRI (voxel size ~1 mm^3), individual folia might be resolved, but significant overlap between representations of body parts should still be expected because of the fractured nature of the homunculus in both lobules V and VIII. fMRI studies that have reported activation in Crus I for sensorimotor tasks did not report any somatotopic organisation (Schlerf et al., 2010; Wiestler et al., 2011), which agrees with microelectrode mapping data (Shambes et al., 1978). While small patches of neurons that specifically respond to stimulation of a body part were reported in Crus I, these patches were not organised somatotopically and measured approximately 0.5 mm in diameter for a rat brain, well below the spatial resolution of an fMRI experiment, leading to severe partial volume effects.

Testing 4 digits in a motor task, a group study at 1.5 T identified ordered clusters of activation for individual digits in ipsilateral lobule V (Grodd et al., 2001), with the highest activated 10 mm^3 of the x digits ordered D1 (thumb)–D3–D2–D5 along the posterior-medial to antero-lateral cerebellar fissures. However, the relatively large voxel size used (3×3×4 mm) may have hindered the exact definition of finger-specific active regions by effectively averaging over several digits. A recent, higher resolution (1.8×1.8×2 mm) study at 3 T (Wiestler et al., 2011) reported a statistically significant somatotopic gradient for four digits in lobule V for a motor task, using multivariate data analysis and cerebellum-specific normalisation (Diedrichsen, 2006). In addition, representations of individual digits (defined by information content) were found in lobules V and VIII for both somatosensory and motor tasks using multivariate data analysis (Wiestler et al., 2011).

Recent increases in field strength used for fMRI led to significant improvements in the spatial resolution of fMRI data because of the increased SNR and BOLD sensitivity (De Martino et al., 2011; van der Zwaag et al., 2009a), also in the cerebellum (Gizewski et al., 2007).

High-resolution, ultra-high field (7 T) fMRI has recently been used successfully to map the individual digit representations in the primary somatosensory cortex (Martuzzi et al., 2012; Sanchez-Panchuelo et al., 2010). The advantage of using high-resolution, 7 T fMRI for the cerebellum has also been demonstrated by two recent studies that identified a motor and a non-motor domain in the cerebellar dentate nucleus (Kuper et al., 2011b) and separate representations for fingers and feet within the motor domain (Kuper et al., 2012), normalizing across subjects specifically for the dentate nucleus to retain spatial resolution (Diedrichsen et al., 2011).

The aim of the present study was thus to map the digit somatotopy in the human cerebellum of individual subjects, using high-resolution fMRI with a somatosensory task, acquiring data at 7 T.

Methods

Data acquisition

Data were collected at a short-bore 7 T MR system (Siemens, Germany) with a head-gradient insert. A quadrature surface coil consisting of a pair of 10 cm diameter loops, which yielded good coverage over the cerebellum and occipital lobe, was used for rf transmission and reception. The use of a local surface coil gives an additional increase in SNR, which can be traded for spatial resolution in fMRI (van der Zwaag et al., 2009b). Similar coils were previously used to acquire very high resolution anatomical images of the cerebellum (Marques et al., 2010b; Marques et al., 2012). fMRI data was acquired using an EPI sequence with sinusoidal readout (Speck et al., 2008) with the following parameters: matrix size: 128×128×36, FOV 154×154 mm^2, leading to a spatial resolution of 1.2×1.2×1.2 mm^3, TR=2500 ms, TE=28 ms, BW/px=1565 Hz/px and $\alpha_{nominal}$=80° in the centre of the cerebellum. The 43 mm thick slab was positioned coronally-oblique so as to cover the entire cerebellum. Three functional runs of 10 min with 240 volumes each were acquired per volunteer.

Anatomical data were acquired using the MP2RAGE sequence (Marques et al., 2010a; Marques et al., 2012) with the following parameters: matrix size=192/180/160, resolution=0.85×0.85×0.85 mm^3, TR$_{mp2rage}$/TE/TI1/TI2=5000 ms/3.75 ms/700 ms/2200 ms. The field of view covered the entire sensitive volume of the rf-coil.

Volunteers and functional paradigms

Ten male, right-handed volunteers (22–33 yrs) participated in this experiment. All subjects provided written informed consent and

the study was approved by the local ethics committee. Data from one volunteer was excluded for a total absence of BOLD signal in the cerebellum. During the experiment, participants were placed in supine position in the scanner with their right arm comfortably stretched along the magnet bore. An experimenter was positioned at the entrance of the bore where he could easily reach and stroke the two distal phalanxes of each digit with his own index finger. The experimenter received auditory cues delivered on MR-compatible headphones (Nordic Neuro Lab, Norway), sent from a local pc using E-prime (Psychology Software Tools, PA). Each digit was independently stroked for 20 s, followed by 10 s of rest (no stroking). During the 20 s of stimulation, the two distal phalanges of each finger were repeatedly stroked along the axis of the finger, from the proximal to the distal portion of the finger. The order in which the digits were stroked was: D1 (thumb), D3 (middle), D5 (little), D2 (index), D4 (ring). This sequence was repeated four times, resulting in a scan time of 10 min per run. Two 'digit' runs were acquired per participant. In a third run, the forearm and palm of the subjects were stroked alternately (20 s of stroking followed by 10 s of rest), with ten repeats per run, again resulting in a scan time of 10 min for the run. The skin surface stroked was larger for the hand and arm than for the digits. To minimize the variability of the stroking procedure, all the stimulations were performed by the same experimenter, keeping similar pace and pressure on the stimulated body parts across subjects. Each stroke had a duration of approximately 700 ms and digits were stroked at a frequency of approximately 1 Hz, leading to some 20–25 strokes per stimulation block. The order of digits stroked was kept constant to avoid human errors by the investigator performing the stroking. No benefits were expected from randomisation of the relatively long stimulus blocks (20 s) as the digit-to-be-stroked was known to the volunteers from the first stroke of the block.

This human touch stimulus was chosen because somatosensory stimuli were also used for the landmark studies by Adrian (Adrian, 1943) and Snider (Snider and Stowell, 1944) and they elicit strong, sustained cerebellar responses (Shambes et al., 1978). Human touch forms a strong somatosensory stimulus, as it supplies complex, natural tactile input and is of major importance for the motor–somatosensory feedback in which the cerebellum is involved. Features such as motion, texture and temporal variability aid in engaging subject attention. In addition, the same stimulus has been used for somatotopic mapping of the primary somatosensory cortex (SI) (Martuzzi et al., 2012) and thus allows comparisons between the obtained cerebellar and SI digit label maps.

Data processing

All fMRI data processing was done in SPM8 (Wellcome Trust Center for Neuroimaging, London, UK) for individual subjects. Pre-processing included the following steps: realignment, smoothing with a Gaussian of FWHM 2 mm and co-registration to the anatomical MP2RAGE image. The GLM model was defined as boxcars convolved with the canonical haemodynamic response, with one regressor per digit, and the motion parameters as nuisance regressors.

Subsequently, for the finger labelling procedure, an f-test (p<0.001) over all five digit regressors (stroking against rest) was used to define a functional mask. Within this mask, each voxel was labelled with the number of the digit that had yielded the highest t-value for this voxel. Note that the winner-takes-all approach does not yield true representations as defined in (Diedrichsen et al., 2012), because only the maximum responding digit is indicated. Thus, clusters of voxels so ascribed to a given digit are referred to as "digit patches". For the hand/arm labelling procedure, a similar approach was used: an f-test over both hand and arm defined voxels of interest, followed by a labelling as hand or arm patch according to the highest t-value for each voxel. All label maps are shown displayed overlaid on the anatomical MP2RAGE images.

Inter-digit distances in lobules V and VIII were calculated as the Euclidian distance between the centres of the digit patches in the label map. Centre locations were defined as the average position of voxels labelled with a given digit number.

A measure of the direction of the somatotopic gradient was obtained via a multivariate linear regression between the digit number and the x, y and z coordinates of the centres of mass of the individual digit patches and subsequent normalisation of the resulting vectors. This approach assumes equal spacing of the digit patches, which seems justified given that no significant differences in digit patch size were found (see Results). Voxel coordinates were taken in the space of the anatomical image, which was acquired purely sagittally, to improve inter-subject comparability of the direction vectors. The R^2 (coefficient of determination) was used as a goodness of fit measure and a two-tailed t-test was used to determine if the somatotopic gradient was significantly different from zero (Prism 5, GraphPad).

To determine the amount of cross-finger responsiveness in the digit patches in lobules V and VIII, parameter estimates (beta values) for stimulation of each of the five digits were extracted from all five digit ROIs. The ROIs were defined as the regions labelled with a given digit number. The contiguous active regions in lobules V and VIII and Crus I were selected with the aid of the Marsbar toolbox in SPM (Brett et al., 2002).

Results

Activation in the ipsilateral cerebellar hemisphere was found in lobule V for all 9 subjects and in lobule VIII for 7 subjects. No activation was found in the contra-lateral cerebellar hemispheres in lobule V or VIII, although some bilateral activation was found in Crus I for all subjects. Example data from a single subject with these three lobules outlined on the anatomy are presented in Fig. 1B. Other lobules also showed active regions (Fig. 1), but these were small and not consistent across subjects and were not further analysed. No activation was found in the dentate nucleus or interposed nucleus, probably because the TE used here (28 ms) was optimised for the cerebellar cortex and the dentate nucleus has a significantly shorter T_2^* (Kuper et al., 2012). In the following paragraphs, digit patches in lobule V will be reported first followed by those in lobule VIII and Crus I. Finally the comparison of the cerebellar digit patches with respect to the hand and arm patches is presented.

Lobule V

Within lobule V, 7 subjects showed a full somatotopic gradient with roughly ordered patches of all 5 digits. Of the two volunteers that did not show a full somatotopic gradient, in one subject lobule V contained an orderly sequence of 4 digit patches (volunteer #2), while for the other subject (#8) only a single finger (thumb) patch was found in lobule V with this digit labelling method (For details, see Table 1). Fig. 2 displays, for all individual subjects, one representative sagittal slice of the label maps that traversed lobule V, overlaid on a slice of the MP2RAGE image. White circles indicate the approximate location of lobule V. In all subjects, the orientation of digits roughly followed an order of D1 to D2, D3, D4 and D5 with D1 most posterior and D5 most anterior, following the orientation of the fissures. This alignment of the somatotopic gradient with the fissures is visible in the axial planes shown in Fig. 3. There were no significant differences in the size of the different digit patches. The size of a single digit patch in lobule V was 110 ± 20 voxels (mean $\pm$ sem, standard error of the mean over subjects), equivalent to 190 ± 30 mm^3 at the used statistical threshold. The Euclidian distance between the centres of adjacent digit representations was 3.7 ± 0.3 mm, which at this spatial resolution means that digit representations could be clearly

Table 1
Orientation of somatotopic gradients in lobule V per individual subject. Subject numbers match those in Fig. 2. The column "orientation gradient" indicates the orientation of the somatotopic gradient in words; the column "orientation gradient vector" gives the result of the multivariate linear regression between digit numbers and coordinates. The value for the most important axis is given in bold text. ml = medial–lateral, pa = anterior–posterior, is = inferior–superior. R^2 is the coefficient of determination for the multivariate linear regression between digit numbers and coordinates. Higher numbers indicate a more linear somatotopic gradient. p-Values in the last column indicate the significance of the slope, *indicates a significantly non-zero slope ($p < 0.05$). The value for the major axis of the somatotopic gradient is given in bold text.

Volunteer	Digit patches	Orientation gradient D1–5	Orientation gradient D1–5 (vector ml, pa, is)	R^2	p-Value axis ml/pa/is
1	1,2,3,4,5	Post → Ant	−0.04 **0.99** 0.11	0.81	0.70/**0.02***/0.41
2	1,2,3,5	Post Inf → Ant Sup	0.23 0.57 **0.79**	0.88	0.07/**0.01***/0.08
3	1,2,3,4,5	Post → Ant	0.11 **0.98** −0.18	0.53	0.75/**0.03***/0.65
4	1,2,3,4,5	Post → Ant	0.09 **0.97** −0.23	0.47	0.83/**0.04***/0.57
5	1,2,3,4,5	Post → Ant	−0.17 **0.91** 0.36	0.63	0.36/**0.07**/0.21
6	1,2,3,4,5	Post Med → Ant Lat	0.21 **0.96** 0.20	0.80	0.19/<**0.01***/0.40
7	1,2,3,4,5	Post Inf → Ant Sup	0.44 **0.65** 0.62	0.58	0.15/**0.09**/0.17
8	1	–	–	–	
9	1,2,3,4,5	Post Med → Ant Lat	0.13 **0.93** 0.34	0.91	0.37/<**0.01***/0.01

distinguished, even though the label maps may have been affected by partial volume effects. The multivariate linear regression between the digit number associated with a voxel and its x, y and z coordinates confirmed a linear somatotopic gradient in the posterior–anterior direction for all volunteers, with an average R^2 value of 0.70 ± 0.06 (mean ± sem). The gradient along the posterior-anterior axis was significantly different from zero ($p < 0.05$) in 6 out of the 8 subjects showing multiple digit patches and showed a strong trend towards significance ($p < 0.10$) in the remaining two (Table 1).

To estimate the degree of partial volume effects and/or neural cross-digit responses, the parameter estimates (beta values) for each of the five digit regressors were extracted from all five digit ROIs (Fig. 4). Because of the manner in which digit regions were defined, the main digit response was always significantly stronger than that of the other digits. Significant responses, of up to 50% of that of the main digit, were also found for neighbouring digits. However, cross-finger responses decreased with the distance to the main digit. For digits that were 3–4 digits apart (for example the response of the D4 ROI to
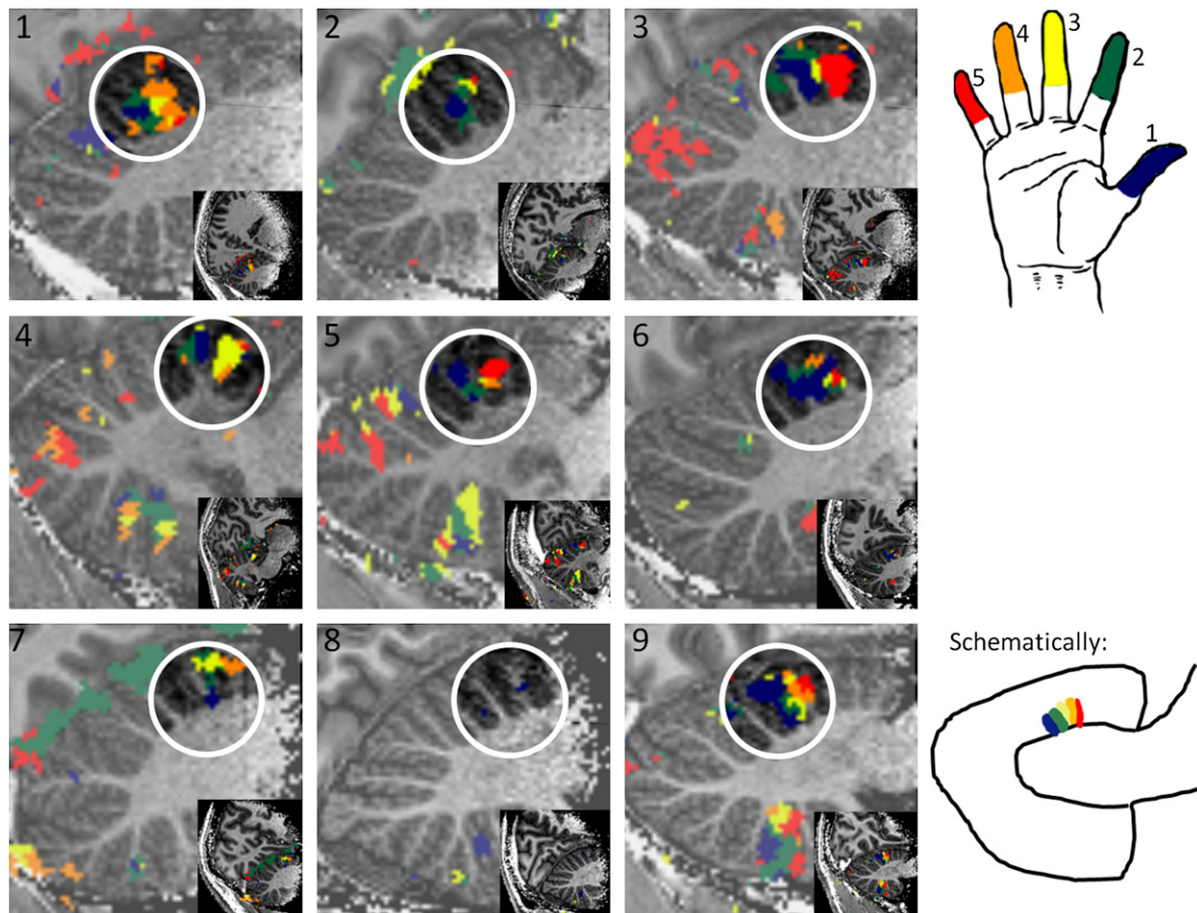

Fig. 2. Examples of somatotopic gradients in lobule V of individual subjects. Label maps are shown overlaid on the MP2RAGE images. Slices shown are sagittal, passing through lobule V at the location where the maximum number of digit patches was visible. The white circle indicates the approximate location of lobule V. Note the high inter-subject variability in cerebellar anatomy. Right-bottom corner: a generalised, schematic drawing of the pattern of the label maps in lobule V of the cerebellum. Blue = thumb/digit 1, green = index finger/digit 2, yellow = middle finger/digit 3, orange = ring finger/digit 4, and red = little finger/digit 5. Subject numbers are stated in black and used consistently throughout.

the stimulation of D1), responses were not significantly different from zero, confirming the local somatotopic organisation.

Lobule VIII

Seven of the nine subjects showed significant activation in lobule VIII (two subjects' data yielded no BOLD signal in the posterior lobe because of low local SNR, likely due to differences in individual anatomy and the resulting insufficient coverage of the rf-coil in the posterior cerebellum). Of the seven subjects that did show activation, six presented an orderly pattern of digit patches (see Table 2). This somatotopic gradient was confirmed by the multivariate linear regression between the digit number and its centre of mass coordinates, but was more variable in orientation than in lobule V, the R^2 values were lower (0.55 ± 0.09, mean $\pm$ sem) than for the somatotopic gradients in lobule V and significance was only reached in four subjects (Table 2). The gradient ran approximately superior–inferior in two subjects (#4 and #6, thumb superior) and in the inferior–superior direction in two other subjects (#5 and #9, thumb inferior), while the remaining two subjects (#7 and #8) showed an incomplete somatotopic gradient (D1–D2–D3–D5), which ran approximately in the medial–lateral (#7) or anterior–posterior (#8) directions. Example slices from these datasets are shown in Fig. 5. The average size of single digit patches in lobule VIII was 60 ± 10 voxels (mean $\pm$ sem), corresponding to 100 ± 17 mm^3 at the used statistical threshold. Single digit patches were thus significantly smaller in lobule VIII than in lobule V (*t*-test, p $=0.01$). The Euclidian distance between the centres of mass of the digits was similar to that found for lobule V; 3.5 ± 0.4 mm.

Extraction of the beta values for all digit patches present in lobule VIII (Fig. 6) led to similar trends as for lobule V, albeit with higher cross-finger responsiveness. Cross-finger responses of up to 65% of the response for the main digit were found for neighbouring digits and clearly lower responses for digits further apart from the target digit, again confirming the somatotopic arrangement of the cerebellar single digit patches.

Crus I

BOLD responses to skin stroking were also consistently detected in Crus I, but, as expected from previous animal (Shambes et al., 1978) and human studies (Wiestler et al., 2011), no somatotopic organisation of digit patches was observed in any of the subjects. Activation was more widespread than in lobules V and VIII and was highly variable between subjects (See Fig. 2, subjects #3, #4 and #5 for examples). The mean size of the active regions was 230 ± 90 voxels equivalent to 390 ± 160 mm^3 at the used statistical threshold. There was no significant difference between the left and the right cerebellar hemispheres.

Hand regions

Stroking of the palm of the hand also resulted in consistent regions of activation. The cerebellar hand patch overlapped with all five digit patches in lobules V and VIII for all subjects that showed BOLD activation (Fig. 7). In addition, the hand region extended both to the anterior and posterior of the digit region in lobule V for all nine subjects. Using a p-value of 0.001 for the mask, the average size of the hand region was 1100 ± 250 mm^3 (mean $\pm$ sem over subjects) in lobule V and 570 ± 100 mm^3 in lobule VIII. A hand region was also found in Crus I; the mean size was 280 ± 90 mm^3. Stroking of the forearm resulted only in scattered voxels, without much consistency between subjects.

Discussion

The degree of somatotopic organisation of the body representation in the cerebellum has long been a point of discussion. The present study shows that while the digit patches in lobules V and VIII show some somatotopic organisation, those in Crus I do not and that the hand patch overlaps with the digit patches in a non-somatotopic manner in both lobules V and VIII.

Methodological considerations

The very small size of the single digit representations and the high inter-subject variability in cerebellar anatomy, evident from the anatomical background slices presented in Fig. 2, required the use of single-subject analysis and a high spatial resolution to robustly separate the digit patches. In the present study, high spatial resolution was achieved by the use of ultra-high field fMRI and a local surface coil for rf-transmission and reception. Ultra-high field fMRI and the use of local surface coils both increase BOLD sensitivity (Gizewski et al., 2007; van der Zwaag et al., 2009a). In addition, the use of a local surface coil allows acquiring images with a reduced field-of-view to increase the spatial resolution (van der Zwaag et al., 2009b; Yacoub et al., 2008) without the SNR or SAR constraints of other reduced FOV techniques (Heidemann et al., 2012; Pfeuffer et al., 2002). This high resolution was essential as the inter-digit distances found for the
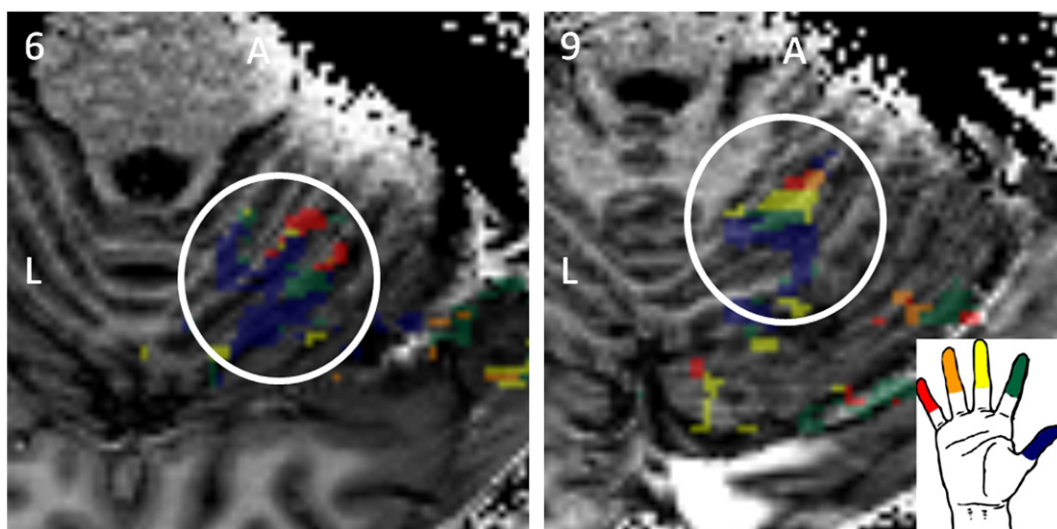

Fig. 3. Axial slices through lobule V for two individual subjects (6 and 9 in Fig. 2). The somatotopic gradient in the label maps follows the direction of the grey-white matter anatomic structure of the fissures visible in the MP2RAGE image. To visualise the underlying anatomy, the labels are shown 50% opaque. The white circle indicates the approximate location of lobule V.
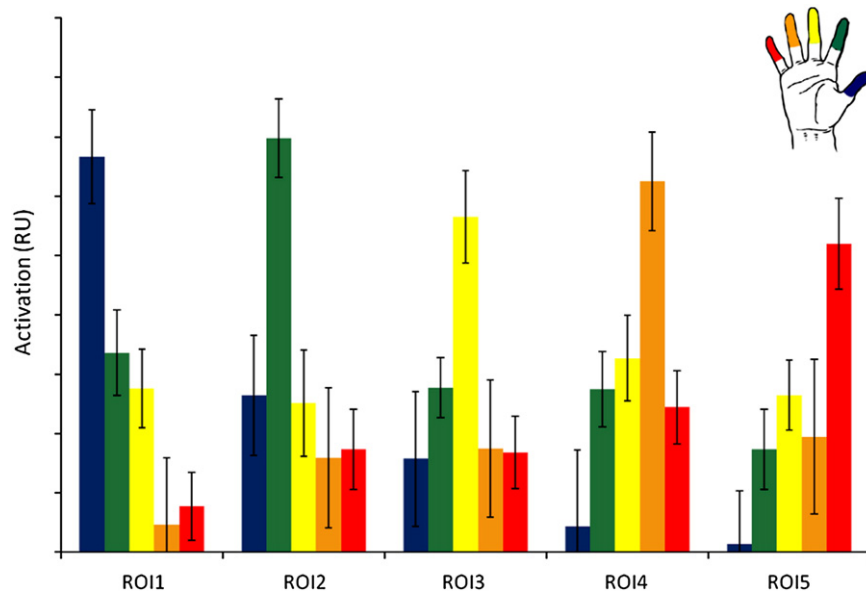
Fig. 4. Beta values extracted for the five digits, for each digit region within lobule V. Digit regions were defined from the label maps in lobule V. ROI1 is the thumb ROI, ROI2 is the index finger ROI, etc. Colours of the responses match those in Figs. 2 and 3: Blue = thumb, green = index finger, yellow = middle finger, orange = ring finger, red = little finger. Error bars indicate the standard error of the mean.

cerebellar digit patches in this study (3.5 mm) are even smaller than inter-digit distances found in BA3b in the primary somatosensory cortex, of 4.2 mm in one study (Sanchez-Panchuelo et al., 2010), 4.5 mm in another (Martuzzi et al., 2012) and 5 mm in a third (Wiestler et al., 2011). Wiestler et al. also showed that separation between digit representations was larger for the primary somatosensory cortex than for lobule V, both for a somatosensory and a motor task (Wiestler et al., 2011).

To improve separation of the individual digits, data were post-processed using a single-subject analysis, allowing application of minimal (2 mm) spatial smoothing. A winner-takes-all approach was used for the generation of the label maps, where each voxel was assigned to a single digit. Subsequently, the sizes of digit patches and the distances between the centres of mass were calculated. While the measured size of the digit regions depends on the threshold chosen to generate the labelling map, the inter-digit distance did not change significantly when different thresholds were used to define the functional mask (see Supplementary Table 1).

Lobule V

Within lobule V, a general finger somatotopic organisation was observed, with the thumb patch most posterior and the little finger most anterior. The orientation of the somatotopic gradient was confirmed with a multivariate linear regression between the digit number associated with a digit patch and the x, y and z coordinates of its centre of mass. The orientation of the somatotopic gradients in lobule V found in this study agrees with those found in previous studies based on motor-task data (Grodd et al., 2001; Wiestler et al., 2011). While Grodd et al. did not report an orderly gradient for the individual fingers, they did observe a postero-medial to antero-lateral orientation of the finger representations, along the cerebellar fissures, as was the case in the present study. Wiestler et al. confirmed the orderly somatotopic gradient observed for a motor task with a statistical test on the centre of gravities of the digit representations across subjects. Interdigit distances reported here for a somatosensory task were slightly larger than those found for the motor task (Wiestler et al., 2011) (3.7 ± 0.4 and <3 mm, respectively).

Although all five digits were identified in lobule V of individual subjects, there were also significant responses for stimulation to neighbouring digits (cross-finger responses). One potential source for cross-finger responses may be that the cerebellar representations of the digits show significant overlap on a much finer anatomical scale; in monkeys, the limb areas were relatively well separated, but within-limb somatotopy was less well defined (Adrian, 1943). This feature was further investigated in rats (Shambes et al., 1978) where a fractured somatotopy was found. As fMRI effectively averages over parts of the mosaic, a single

Table 2
Orientation of somatotopic gradients in lobule VIII per individual subject. Subject numbers match those in Table 1 and Fig. 2. The column "orientation gradient" indicates the orientation of the somatotopic gradient in words; the column "orientation gradient vector" gives the result of the multivariate linear regression between digit numbers and coordinates. The value for the most important axis is given in bold text. ml = medial–lateral, pa = anterior–posterior, is = inferior–superior. R^2 is the coefficient of determination for the multivariate linear regression between digit numbers and coordinates. Higher numbers indicate a more linear somatotopic gradient. p-Values in the last column indicate the significance of the slope, *indicates a significantly non-zero slope ($p < 0.05$). The value for the major axis of the somatotopic gradient is given in bold text.

| Volunteer	Digit patches	Orientation gradient D1–5	Orientation gradient D1–5 (vector ml, pa, is)	R^2	p-Value axis ml/pa/is
1	–	–	–	–	–
2	–	–	–	–	–
3	1,2,3,4,5	Unclear	−0.59 0.37 **0.71**	0.24	**0.29**/0.53/0.40
4	1,2,3,4	Sup→Inf	−0.11 0.24 **−0.96**	0.86	0.59/0.24/**0.03***
5	1,2,3,4,5	Inf→Sup	0.38 0.26 **0.88**	0.80	0.91/0.08/**<0.01***
6	1,2,3,4,5	Sup Lat→Inf Med	−0.55 0.20 **−0.80**	0.65	**0.02***/0.26/0.12
7	1,2,3,5	Med Post→Lat Ant	**0.74** 0.52 0.40	0.29	**0.17**/0.61/0.52
8	1,2,3,5	Ant Sup→Post Inf	−0.33 **−0.66** **−0.67**	0.56	0.60/**0.22**/0.52
9	1,2,3,4,5	Inf Post→Sup Ant	0.08 0.53 **0.84**	0.46	0.63/**0.02***/0.25
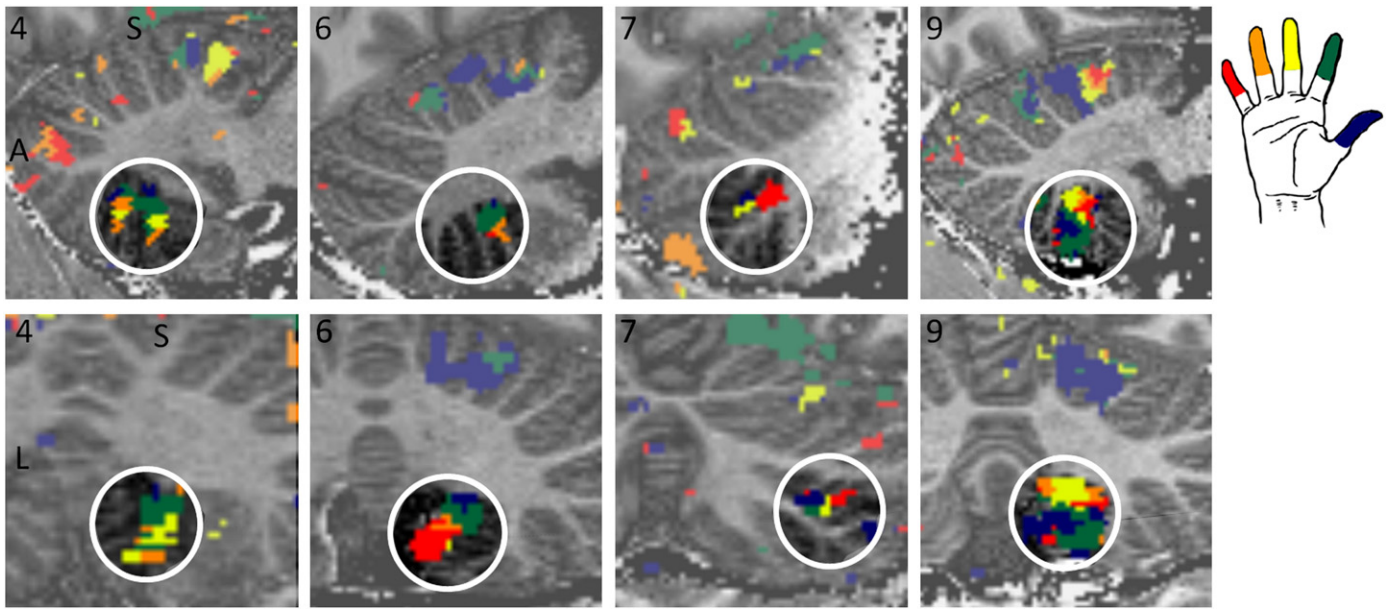
Fig. 5. Label maps in lobule VIII for 4 individual subjects (4, 6, 7 and 9 in Fig. 2/Tables 1 and 2). Presented slices were selected to show the maximum number of digits in one slice. The top row displays a sagittal slice for each subject while the bottom row displays coronal slices for the same subjects. Subject 4 displays a superior–inferior somatotopic gradient (D1 to D5) and subject 6 a superiolateral–inferiomedial gradient, while subject 7 presented a somatotopic gradient which was oriented posteromedial to anterolateral and subject 9 displayed an inferior–superior gradient. S = superior, A = anterior, L = left. White circles indicate the approximate location of lobule VIII. Subject numbers are given in black.

digit may be dominating the cerebellar tissue covered by a voxel, but this voxel may also contain patches corresponding to other fingers, or indeed, to the hand. Alternatively, substantial partial volume effects may remain, as digit patches contain a relatively low number of voxels. These partial volume effects might also contribute to the cross-finger responsiveness seen for neighbouring digits.

Comparing the cross-digit responses of cerebellar digit patches in lobule V to those of the digit patches in Brodmann area (BA) 3b of the primary somatosensory cortex, it is clear that the digits in BA3b are much more separated spatially (Martuzzi et al., 2012). Responses of neighbouring digits are generally smaller than those reported here and even negative BOLD responses were reported for digits 3–4 digits apart from the digit being stroked. The difference in voxel size (2.2 μl in the SI study vs. 1.7 μl here) and reported size of digit regions in the

two studies is not sufficient to explain this difference in cross-finger responsiveness. Also, BA2 of the primary somatosensory cortex, which is known to integrate more somatosensory information than BA3b (Gardner and Costanzo, 1980), shows a degree of overlap which is more comparable to that seen here in cerebellar lobule V (Martuzzi et al., 2012). Thus, the relatively high level of cross-finger responsiveness may indicate a higher level of integration of the somatosensory information in the cerebellum rather than simple partial volume effects.

Lobule VIII

To the best of our knowledge, no previous human fMRI study has reported a somatotopic organisation in lobule VIII. We observed a
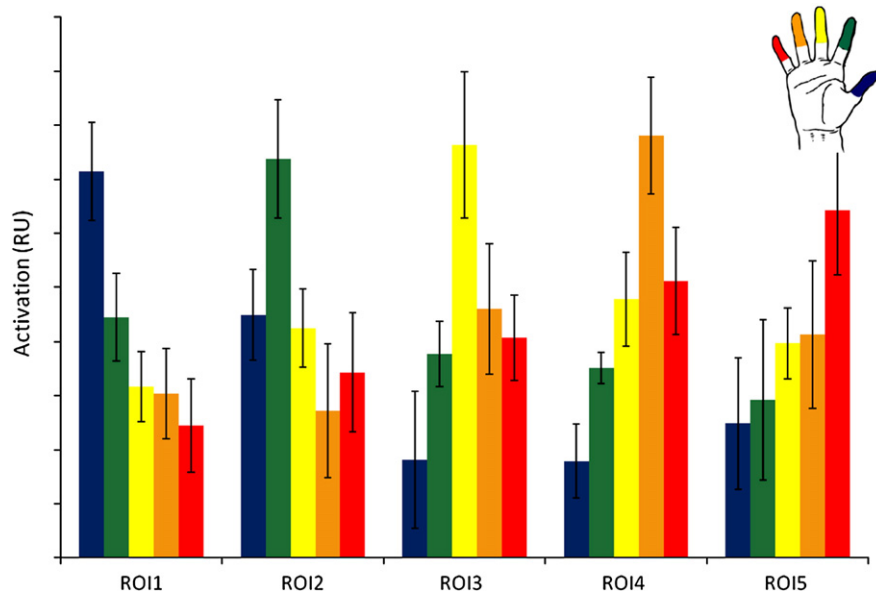

Fig. 6. Beta values extracted for the five digits, for each digit region within lobule VIII. Digit regions were defined from the label maps in lobule VIII. ROI1 is the thumb ROI, ROI2 is the index finger ROI, etc. Error bars indicate the standard error of the mean.
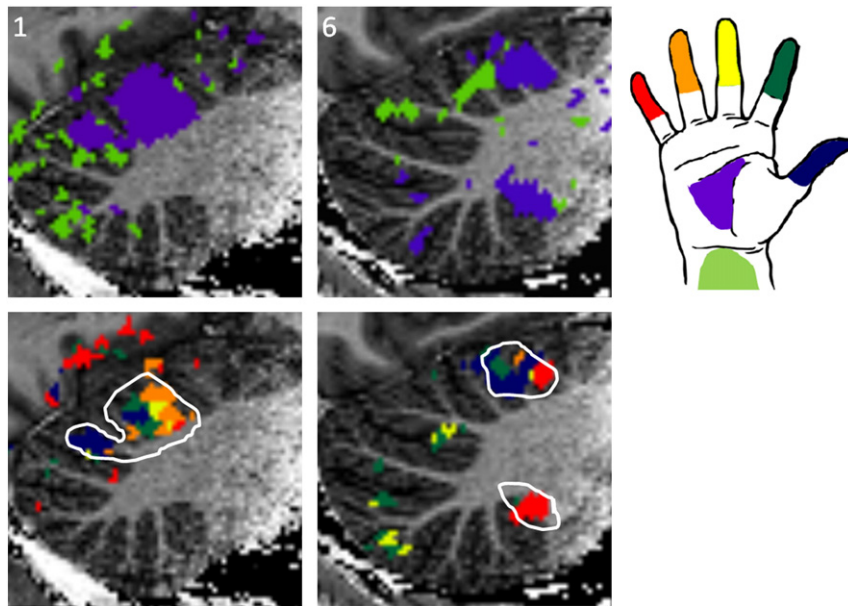
Fig. 7. Hand/arm label maps. Purple = hand, light green = forearm. a/c Hand/arm label maps from two representative individual subjects (1 and 6 in Fig. 2/Tables 1 and 2). b/d For comparison, the digit label map is shown with the outline of the hand patch. The hand region overlapped with all the digit regions in both lobules V and VIII. Arm stroking resulted in only small scattered regions of 'activation'.

higher inter-subject variability in the orientation of the somatotopic gradient in lobule VIII than in lobule V (Fig. 5, Tables 1 and 2). Such varied gradients can only be observed in a single-subject processing approach, because the underlying anatomy is highly complex (Diedrichsen, 2006) and not completely preserved in a normalisation process. The presence of a somatotopic gradient in lobule VIII was confirmed by the analysis of local beta values, which showed a decreasing response for digits further apart in lobule VIII, similar to results in lobule V. Increased inter-subject variability in lobule VIII has also been reported for a motor task (Table 2 (Wiestler et al., 2011)), where a reduced systematic spatial ordering of finger representations across subjects was found in lobule VIII compared to lobule V and the primary somatosensory cortex.

Cross-finger responses were higher in lobule VIII than in lobule V. This agrees with the increased overlap between the cerebellar representations of neighbouring body parts in lobule VIII compared to lobule V, as reported by Snider and Stowell in micro-electrode mapping of the cat cerebellum (Snider and Stowell, 1944). Thus, the explanation for the increased overlap is probably of biological origin and may indicate a higher degree of cooperation between the local neural substrates of the digits. However, it cannot be ruled out that the increased cross-digit responses may also be due to the smaller size of the digit patches and the consequently increased partial volume effects.

If the difference in cross-digit activation levels between lobule V and lobule VIII is due to a higher degree of signal integration in lobule VIII, this may arise from the different function of the relevant lobules during somatosensory stimulation. A functional difference between lobule V and VIII has been proposed (Glickstein et al., 2011) where the lobule V of the anterior cerebellum, SMA and the prefrontal cortex form a preparatory loop, with activity preceding the action and lobule VIII as part of an executive network, together with the motor cortex and thalamus. Cerebellar lesions in either lobule V or VIII also result in slightly different impairments in hand movements (Kuper et al., 2011a).

Crus I

Regions in Crus I responded to tactile stimulation, but activations did not show a somatotopic organisation. Although Crus I is not usually thought of as a cerebellar sensorimotor area, neural connections from the forelimb to the Crus I area have been demonstrated in macaque monkey using retrograde tracer methods (Lu et al., 2007). Activation in Crus I of similar size to that reported here was also reported by Wiestler et al. for a vibrotactile stimulus applied to the finger tips and agrees with our observation that this activation is not somatotopically organised (Wiestler et al., 2011). It has previously been suggested that the neocerebellum is involved in complex motor tasks (Schlerf et al., 2010) and the results presented here suggest it might also be involved in processing of complex somatosensory stimuli. Comparing the human touch to mechanical stimulation of the individual fingers or hand should allow the investigation of the influence of stimulus type on the BOLD response in the individual lobules.

Hand region

Cerebellar hand patches spanned the entire digit region and further extended posteriorly and anteriorly in most subjects. From the fMRI data, one cannot distinguish if these hand and digit regions overlap on a neural scale or whether the 'overlay' is caused by a finely interleaved somatotopy of the hand and digits as in a fractured somatotopy. A similar, non-somatotopic, pattern of the hand representation surrounding and incorporating digit representations has been reported for the primary motor cortex in both humans (Meier et al., 2008; Sanes et al., 1995) and macaques (Park et al., 2001). This fractured somatotopy and the close intermingling of hand and digit neurons are thought to improve the cooperation between hand and finger muscles (Sanes et al., 1995; Shambes et al., 1978). It is interesting to note that such intermingling is also found in the cerebellum for a somatosensory task, perhaps because of the importance of the cerebellar regions in the somatomotor feedback loop.

One study that investigated the use of winner-takes-all labelling maps in the primary motor cortex (Meier et al., 2008) found a hand region which extended both superior and inferior to the digit representations. They then demonstrated that if a winner-takes-all approach including hand and forearm is used to generate a label map, dual hand and forearm regions appear, as the central part of the hand and arm representations is assigned to the digits. Thus, inclusion of hand and arm activation in the labelling approach may impair understanding of the layout of these regions relative to one another.

Conclusion

We conclude that high resolution fMRI acquired at 7 T using a surface coil, can map individual digits in the human cerebellum with a somatosensory stimulus. The digit patches located in lobule V, lobule VIII and Crus I were characterized by different degrees of somatotopic organisation. Somatotopic organisation in individual subjects showed greatest somatotopy in lobule V, was less constant in lobule VIII, and absent in Crus I. Anatomically, the somatotopic gradient in lobule V was consistently in the posterior (D1) to anterior (D5) direction, while the direction of the gradient in lobule VIII differed between subjects. A comparison with the hand region revealed that the digit regions in lobules V and VIII completely overlapped with the palmar hand patch. These data suggest that the body representations in the cerebellum are only partially somatotopically organised in humans, similar to what was observed previously in invasive studies in animals.

Supplementary data to this article can be found online at http://dx.doi.org/10.1016/j.neuroimage.2012.11.041.

Acknowledgments

References

Adrian, E.D., 1943. Afferent areas in the cerebellum connected with the limbs. Brain 66, 289–315.

Brett, M., Anton, J.L., Valabregue, R., Poline, J.P., 2002. Region of interest analysis using an SPM toolbox. Presented at the 8th International Conference on Functional Mapping of the Human Brain [abstract], Sendai, Japan.

Buckner, R.L., Krienen, F.M., Castellanos, A., Diaz, J.C., Yeo, B.T., 2011. The organization of the human cerebellum estimated by intrinsic functional connectivity. J. Neurophysiol. 106, 2322–2345.

De Martino, F., Esposito, F., Van de Moortele, P.F., Harel, N., Formisano, E., Goebel, R., Ugurbil, K., Yacoub, E., 2011. Whole brain high-resolution functional imaging at ultra high magnetic fields: an application to the analysis of resting state networks. Neuroimage 57, 1031–1044.

Diedrichsen, J., 2006. A spatially unbiased atlas template of the human cerebellum. Neuroimage 33, 127–138.

Diedrichsen, J., Maderwald, S., Kuper, M., Thurling, M., Rabe, K., Gizewski, E.R., Ladd, M.E., Timmann, D., 2011. Imaging the deep cerebellar nuclei: a probabilistic atlas and normalization procedure. Neuroimage 54, 1786–1794.

Diedrichsen, J., Wiestler, T., Krakauer, J.W., 2012. Two distinct ipsilateral cortical representations for individuated finger movements. Cereb. Cortex. http://dx.doi.org/10.1093/cercor/bhs120 (Epub ahead of print).

Gardner, E.P., Costanzo, R.M., 1980. Spatial integration of multiple-point stimuli in primary somatosensory cortical receptive fields of alert monkeys. J. Neurophysiol. 43, 420–443.

Gizewski, E.R., de Greiff, A., Maderwald, S., Timmann, D., Forsting, M., Ladd, M.E., 2007. fMRI at 7 T: whole-brain coverage and signal advantages even infratentorially? Neuroimage 37, 761–768.

Glickstein, M., Sultan, F., Voogd, J., 2011. Functional localization in the cerebellum. Cortex 47, 59–80.

Granziera, C., Schmahmann, J.D., Hadjikhani, N., Meyer, H., Meuli, R., Wedeen, V., Krueger, G., 2009. Diffusion spectrum imaging shows the structural basis of functional cerebellar circuits in the human cerebellum in vivo. PLoS One 4, e5101.

Grodd, W., Hulsmann, E., Lotze, M., Wildgruber, D., Erb, M., 2001. Sensorimotor mapping of the human cerebellum: fMRI evidence of somatotopic organization. Hum. Brain Mapp. 13, 55–73.

Heidemann, R.M., Ivanov, D., Trampel, R., Fasano, F., Meyer, H., Pfeuffer, J., Turner, R., 2012. Isotropic submillimeter fMRI in the human brain at 7 T: combining reduced field-of-view imaging and partially parallel acquisitions. Magn. Reson. Med. 68 (5), 1506–1516. http://dx.doi.org/10.1002/mrm.24156.

Kuper, M., Brandauer, B., Thurling, M., Schoch, B., Gizewski, E.R., Timmann, D., Hermsdorfer, J., 2011a. Impaired prehension is associated with lesions of the superior and inferior hand representation within the human cerebellum. J. Neurophysiol. 105, 2018–2029.

Kuper, M., Dimitrova, A., Thurling, M., Maderwald, S., Roths, J., Elles, H.G., Gizewski, E.R., Ladd, M.E., Diedrichsen, J., Timmann, D., 2011b. Evidence for a motor and a non-motor domain in the human dentate nucleus — an fMRI study. Neuroimage 54, 2612–2622.

Kuper, M., Thurling, M., Stefanescu, R., Maderwald, S., Roths, J., Elles, H.G., Ladd, M.E., Diedrichsen, J., Timmann, D., 2012. Evidence for a motor somatotopy in the cerebellar dentate nucleus — an fMRI study in humans. Hum. Brain Mapp. 33 (11), 2741–2749.

Lu, X., Miyachi, S., Ito, Y., Nambu, A., Takada, M., 2007. Topographic distribution of output neurons in cerebellar nuclei and cortex to somatotopic map of primary motor cortex. Eur. J. Neurosci. 25, 2374–2382.

Manto, M., Bower, J.M., Conforto, A.B., Delgado-Garcia, J.M., da Guarda, S.N., Gerwig, M., Habas, C., Hagura, N., Ivry, R.B., Marien, P., Molinari, M., Naito, E., Nowak, D.A., Oulad Ben Taib, N., Pelisson, D., Tesche, C.D., Tilikete, C., Timmann, D., 2012. Consensus paper: roles of the cerebellum in motor control — the diversity of ideas on cerebellar involvement in movement. Cerebellum 11, 457–487.

Marques, J.P., Kober, T., Krueger, G., van der Zwaag, W., Van de Moortele, P.F., Gruetter, R., 2010a. MP2RAGE, a self bias-field corrected sequence for improved segmentation and T1-mapping at high field. Neuroimage 49, 1271–1281.

Marques, J.P., van der Zwaag, W., Granziera, C., Krueger, G., Gruetter, R., 2010b. Cerebellar cortical layers: in vivo visualization with structural high-field-strength MR imaging. Radiology 254, 942–948.

Marques, J.P., Gruetter, R., van der Zwaag, W., 2012. In vivo structural imaging of the cerebellum, the contribution of ultra-high fields. Cerebellum 11, 384–391.

Martuzzi, R., van der Zwaag, W., Farthouat, J., Gruetter, R., Blanke, O., 2012. Human finger somatotopy in areas 3b, 1, and 2: a 7 T fMRI study using a natural stimulus. Hum. Brain Mapp. http://dx.doi.org/10.1002/hbm.22172 (Epub ahead of print).

Meier, J.D., Aflalo, T.N., Kastner, S., Graziano, M.S., 2008. Complex organization of human primary motor cortex: a high-resolution fMRI study. J. Neurophysiol. 100, 1800–1812.

Park, M.C., Belhaj-Saif, A., Gordon, M., Cheney, P.D., 2001. Consistent features in the forelimb representation of primary motor cortex in rhesus macaques. J. Neurosci. 21, 2784–2792.

Pfeuffer, J., van de Moortele, P.F., Yacoub, E., Shmuel, A., Adriany, G., Andersen, P., Merkle, H., Garwood, M., Ugurbil, K., Hu, X., 2002. Zoomed functional imaging in the human brain at 7 tesla with simultaneous high spatial and high temporal resolution. Neuroimage 17, 272–286.

Rijntjes, M., Buechel, C., Kiebel, S., Weiller, C., 1999. Multiple somatotopic representations in the human cerebellum. Neuroreport 10, 3653–3658.

Sanchez-Panchuelo, R.M., Francis, S., Bowtell, R., Schluppeck, D., 2010. Mapping human somatosensory cortex in individual subjects with 7 T functional MRI. J. Neurophysiol. 103, 2544–2556.

Sanes, J.N., Donoghue, J.P., Thangaraj, V., Edelman, R.R., Warach, S., 1995. Shared neural substrates controlling hand movements in human motor cortex. Science 268, 1775–1777.

Schlerf, J.E., Verstynen, T.D., Ivry, R.B., Spencer, R.M., 2010. Evidence of a novel somatopic map in the human neocerebellum during complex actions. J. Neurophysiol. 103, 3330–3336.

Schmahmann, J.D., Doyon, J., McDonald, D., Holmes, C., Lavoie, K., Hurwitz, A.S., Kabani, N., Toga, A., Evans, A., Petrides, M., 1999. Three-dimensional MRI atlas of the human cerebellum in proportional stereotaxic space. Neuroimage 10, 233–260.

Shambes, G.M., Gibson, J.M., Welker, W., 1978. Fractured somatotopy in granule cell tactile areas of rat cerebellar hemispheres revealed by micromapping. Brain Behav. Evol. 15, 94–140.

Snider, R.S., Stowell, A., 1944. Receiving areas of the tactile, auditory and visual systems in the cerebellum. J. Neurophysiol. 7, 331–358.

Speck, O., Stadler, J., Zaitsev, M., 2008. High resolution single-shot EPI at 7 T. MAGMA 21, 73–86.

Stoodley, C.J., Schmahmann, J.D., 2009. Functional topography in the human cerebellum: a meta-analysis of neuroimaging studies. Neuroimage 44, 489–501.

Stoodley, C.J., Schmahmann, J.D., 2010. Evidence for topographic organization in the cerebellum of motor control versus cognitive and affective processing. Cortex 46, 831–844.

Stringer, E.A., Chen, L.M., Friedman, R.M., Gatenby, C., Gore, J.C., 2011. Differentiation of somatosensory cortices by high-resolution fMRI at 7 T. Neuroimage 54, 1012–1020.

van der Zwaag, W., Francis, S., Head, K., Peters, A., Gowland, P., Morris, P., Bowtell, R., 2009a. fMRI at 1.5, 3 and 7 T: characterising BOLD signal changes. Neuroimage 47, 1425–1434.

van der Zwaag, W., Marques, J.P., Hergt, M., Gruetter, R., 2009b. Investigation of high-resolution functional magnetic resonance imaging by means of surface and array radiofrequency coils at 7 T. Magn. Reson. Imaging 27, 1011–1018.

Wiestler, T., McGonigle, D.J., Diedrichsen, J., 2011. Integration of sensory and motor representations of single fingers in the human cerebellum. J. Neurophysiol. 105, 3042–3053.

Yacoub, E., Harel, N., Ugurbil, K., 2008. High-field fMRI unveils orientation columns in humans. Proc. Natl. Acad. Sci. U. S. A. 105, 10607–10612.